Proceedings 10th NUMGE 2023
10th European Conference on Numerical Methods in Geotechnical Engineering
Zdravkovic L, Kontoe S, Taborda DMG, Tsiampousi A (eds)

https://doi.org/10.53243/NUMGE2023-192

Numerical back analysis of Crossrail Bond Street Station sprayed concrete lined (SCL) concourse tunnel primary lining thickening layer longitudinal cracks

J. Su[1]

[1]*Ramboll, London, UK*

ABSTRACT: The Crossrail Bond Street Station east end concourse tunnel comprises one layer of fibre-reinforced SCL primary lining and one layer of SCL thickening layer, in which steel reinforcement is installed locally around the 4no. cross-passage openings on both sides of the tunnel. After completing the thickening layer and the cross-passages, a deep longitudinal crack was observed at the crown of the thickening layer. The reason for this crack needed to be better understood. This paper aims to address this knowledge gap. This paper first introduces the tunnel layout, lining configuration and construction sequence. This is followed by a qualitative explanation of the reasons for the cracking. The main part of this paper is a presentation of lining stresses results from a numerical back analysis using the finite element package PLAXIS 3D. The analysis considers key influencing factors on the performance of the thickening layer, such as the sequential construction, early-age thermal and shrinkage-induced tensile stress and the impact of the multiple cross-passage constructions. Finally, recommendations are made for the numerical simulation of multi-layer tunnel lining with multiple cross-passage constructions.

Keywords: Numerical analysis; Sprayed concrete; Multi-layer lining; Cross-passages; Tunnel lining cracks

1 INTRODUCTION

Crossrail is an £18.9 billion railway project that links Reading and Heathrow to the West of London and Abbey Wood and Shenfield to the East of London. The central section of Crossrail consists of five underground stations constructed using the SCL method (Su and Thomas 2015). An innovation of Crossrail SCL junction construction was first to build a layer of fibre-reinforced SCL primary lining to support the excavated ground, followed by a steel-reinforced thickening layer designed to resist the concentration of tensile stress for the opening. The two layers of concrete linings are in direct concrete-to-concrete contact. This falls into the fully composite multi-layer lining (MLL) system, as Su (2022a) discussed. The Crossrail Bond Street Station east end concourse tunnel CH3 has adopted this innovative lining configuration around the 4no. cross-passage openings on both sides of the tunnel. After completing the thickening layer and the cross-passages (CPs), a deep longitudinal crack was observed at the crown of the thickening layer, as shown in Figures 1 and 2, respectively (Su et al. 2019). The industry did not sufficiently understand the reason for this crack. This paper aims to address this knowledge gap.

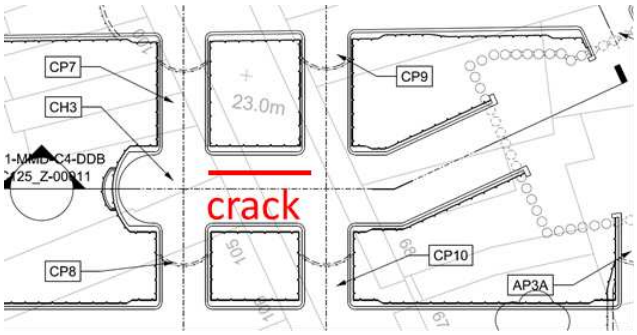

Figure 1. Location of the longitudinal crack in the plan

Figure 2. (left) Location of the longitudinal crack at the crown (right) depth of the crack

2 CROSSRAIL JUNCTION DESIGN

The concourse tunnel CH3 is around 10m in diameter from the theoretical excavation line. It was constructed with a 5.3m diameter and 250mm thick primary lining SCL pilot tunnel from the east through to the west end of the CH3, followed by an enlargement using two top headings, a double bench and a double invert construction sequence. The CH3 primary lining, including the initial layer, is 400mm thick. This is followed by a further 350mm thick steel reinforced thickening layer, as shown in Figure 3. The cross-passage SCL tunnels are around 6.6m in diameter from the theoretical excavation line, and the primary lining is 250mm. They used a top heading and an invert excavation sequence constructed from the CH3 towards the two platform SCL tunnels on both sides, as shown in Figure 4.

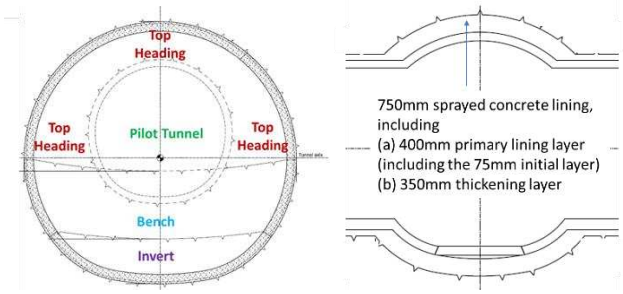

Figure 3. CH3 tunnel cross-section

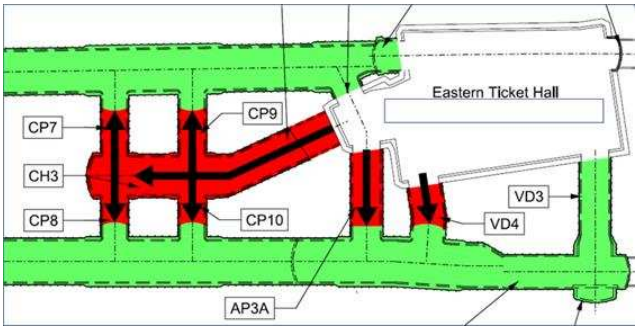

Figure 4. Construction sequence for the CH3

At the early stage of the Crossrail SCL tunnel detailed design, a parametric numerical study was undertaken using the Finite Difference Programme FLAC3D. The study investigated a series of tunnel junctions between a main SCL tunnel and different diameter cross-passage tunnels to understand the impact of the relative tunnel dimension ratio on the stress concentration in the main tunnel. The stress concentration factors and areas requiring steel reinforcement were derived for junctions with different dimension ratios. Using these factors, 3D numerical analyses were avoided for the design of most junctions. Instead, 2D plain strain numerical analyses were carried out for all main tunnels. The hoop force obtained from the 2D analyses was subsequently multiplied by the stress concentration factors to obtain the new set of hoop forces and the bending moment around the junctions for quantifying the amount and area of the steel reinforcement.

3 LIMITATIONS OF CROSSRAIL DESIGN

The Crossrail SCL tunnel junction design represented the most advanced design methodology around the 2010s'. By adopting the stress concentration factor approach, steel reinforcement around most tunnel junctions can be designed without 3D numerical analyses, saving significant resources, cost and time. However, there are some limitations to this approach.

The first limitation is that the Crossrail junction design approach did not consider the effect of sequential construction between the primary lining and the thickening layer. When modelling the construction of the main tunnel CH3, the 400mm thick primary lining and the 350mm thick thickening layer were installed simultaneously using 750mm thick plate elements. This led to both lining layers resisting a similar magnitude of hoop compression. In reality, the primary lining was installed immediately after ground excavation and resisted the short-term ground load and groundwater pressure. Only after completing all primary lining of the CH3 and installing steel reinforcement around the openings, the thickening layer sprayed. At this stage, the thickening layer did not resist any external loads.

The second limitation is that it did not consider the effect of early-age thermal (EAT) and shrinkage (SHK) induced tensile stress in the thickening layer due to the restraint effect from the sprayed concrete primary lining substrate. If the tensile stress is big enough, it could cause lining cracks at the crown.

The third limitation is that the Crossrail junction design approach only covered one junction scenario. If multiple junctions are constructed on both sides of the main tunnel, the changing lining stiffness between the opening area and the non-opening areas may result in different stress distributions in the lining due to soil-structure interaction.

This paper investigates the impact of the first two factors on the observed cracks by undertaking several numerical analyses, as detailed in the next section.

4 NUMERICAL ANALYSIS

4.1 Modelling plan

To illustrate the effect of the three factors mentioned above, this study presents results from the following three models, as shown in Table 1. Model 1 represents the original Crossrail approach, in which the primary lining and the thickening layer are installed in one step without considering any effect of EAT and SHK. Models 2 and 3 represent improved modelling approaches in which the two layers of linings are to be installed sequentially. The impact of EAT and SHK is only considered in Model 3. This study is carried out using the Finite Element Package PLAXIS3D.

Table 1. Modelling plan

Model No.	Sequential construction	EAT & SHK
1	N	N
2	Y	N
3	Y	Y

4.2 Model geometry and boundary conditions

The global model and its mesh, the relative tunnel position and the CH3 pilot and enlargement tunnels are shown in Figures 6-8, respectively. The CH3 axis is approximately 22m below the ground surface. The distances between the CH3 and the two platform tunnels are around 22m. The left and right-hand side CPs were constructed about 5m and 8m, respectively, with a temporary headwall at the end. The rest of the CPs were built from the two SCL platform tunnels, which is outside this study's timeline. The model's vertical boundaries are fixed horizontally. The bottom boundaries are fixed vertically. No ground surface surcharge is assumed in this study. The linings of the two TBM pilot tunnels, the CH3 SCL pilot tunnel and the 4no. CPs are simulated using plate elements. The CH3 primary lining and thickening layer are modelled using volume elements to facilitate the simulation of fully composite action in between. A mesh density sensitivity study was undertaken to balance the result's accuracy and the time spent running the model.

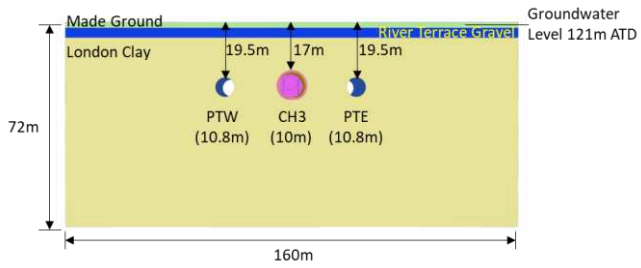

Figure 6: Global model

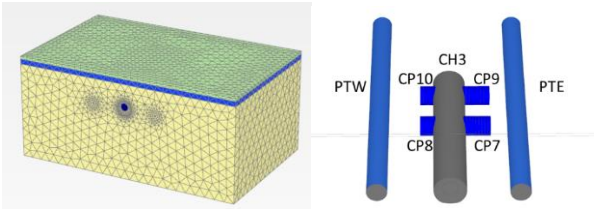

Figure 7: Model mesh and relative position of all tunnels

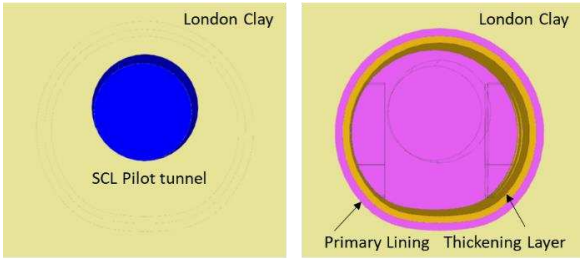

Figure 8: CH3 pilot (left) and enlargement (right) tunnels

4.3 Stratification and geotechnical assumptions

A typical London Basin geological stratification is simulated, as shown in Table 2. Made Ground (MG) and River Terrace Gravel (RTD) are modelled as drained material using Mohr-Coulomb (MC) material model. London Clay (LC) is modelled as an undrained material using an undrained C type of analysis and MC material model. The undrained C type of analysis is a total stress analysis, which does not separate the effective stress and the pore water pressure. It is suitable for this study as all construction activities were completed within a few months when the LC was still undrained. The undrained shear strength profile follows the Crossrail Bond Street Station SCL tunnel design (Bloodworth and Su 2018). The undrained stiffness is assumed using an empirical equation that its value is 400 times the undrained shear strength at the same depth. The groundwater level is assumed at 121m ATD (above tunnel datum), 1m below the ground surface level. The groundwater profile is modelled as hydrostatic.

Table 2. Geological stratigraphy

Material	Top [mATD]	Bottom [mATD]	Thickness [m]
Made ground	122.0	120.0	2.0
River Terrace Deposit	120.0	116.5	3.5
London Clay	116.5	50	66.5

Table 3. Properties of Made Ground and River Terrace Deposit

Material	MG	RTD
Unsaturated unit weight [kNm^{-3}]	16.5	17
Saturated unit weight [kNm^{-3}]	20	20
Coefficient of earth pressure at rest K_0	0.5	0.5
Drained elastic modulus E' [kPa]	10e3	30e3
Effective cohesion c' [kPa]	0	0
Effective friction angle Φ' [deg]	25	38
Drained Poisson's ratio ν'	0.3	0.3

Table 4. Properties of London Clay

Material	LC
Unsaturated unit weight [kNm^{-3}]	20
Saturated unit weight [kNm^{-3}]	20
Coefficient of earth pressure at rest K_0	1.2
Undrained elastic modulus Eu at the reference level [kPa]	28e3
Undrained shear strength Cu at reference level [kNm^{-2}]	70
Reference level	116.5
Increments of undrained elastic modulus Eu with depth [kNm^{-2}/m]	4400
Increments of undrained shear strength Cu with depth [kNm^{-2}/m]	11
Undrained Poisson's ratio ν_u	0.495

4.4 Tunnel construction modelling approach

This section describes the tunnel construction modelling approach in the order of the modelling sequence.

For the two TBM tunnels, the ground within the tunnel is removed and the 300mm thick lining is installed in one step with a prescribed 1.0% volume loss, following the Crossrail design standard (2009).

For CH3 SCL pilot tunnel construction, a simplified two-step modelling approach was used instead of modelling the 1m advance construction sequence. The first step removes the ground within the whole length of the pilot tunnel with a 50% in-situ stress reduction around the tunnel periphery. The second step reduces the remaining 50% in-situ stress to zero and installs the 250mm thick lining for the whole tunnel length.

For CH3 SCL enlargement construction, the same two-step approach was used instead of modelling the two top headings, double bench and double invert advance sequence. This is because the stress condition in the CH3 primary lining does not affect the stress condition of the thickening layer.

The thickening layer is simulated also using volume element and activated at the same stage or the following stage of the primary lining construction. This approach allows the simulation of composite action between the two layers of linings (Su and Bloodworth 2018, 2019, Bloodworth and Su 2018, Su 2022b). It also allows the simulation of the effect of EAT and SHK-induced tensile stress in the thickening layer (Su and Bedi 2019).

For the 4no. CPs, the two top headings and the double invert construction sequence are modelled as 1m full ring advance. This is based on the findings from Su (2022c) that only the top heading construction will relax the ground and induce additional lining forces. The CPs are excavated sequentially in the order of CP8, CP10, CP7 and CP9. All linings are modelled using the linear elastic model with Young's modulus of 17GPa.

5 PRESENTATION AND DISCUSSIONS OF THE RESULTS

5.1 Principal stress results

This section presents the principal compressive or tensile stress when the thickening layer is installed (left-hand side) and at the last stage when all CPs construction is completed (right-hand side). The contour plots are all shown in the direction from the west to the east (i.e. readers look through the headwall into the tunnel).

Figure 9 shows model no.1 principal compressive stress plots for the thickening layer. As the thickening layer is installed at the same stage as the primary lining, ground load and groundwater pressure are partly resisted by the thickening layer. Hence, principal compressive stresses around 1.5-1.8MPa are observed at the crown in Figure 9 (left). After constructing the CPs, the maximum compressive stress occurs at the crown between the opposite CPs and the magnitude is increased to around 2.5-3.0MPa. The minimum compressive stress occurs at the crown between the two shallow blue areas, with the magnitude reduced to around 0.5MPa, as shown in Figure 9 (right). No tensile stress was developed at the crown for both stages.

Figure 10 shows model no.2 principal tensile stress plots for the thickening layer. As the thickening layer is installed at the stage after the primary lining construction, no ground load nor groundwater pressure is resisted by the thickening layer. A very low magnitude of principal tensile stress is developed, as shown in Figure 10 (left). This is caused entirely by its self-weight. After constructing CPs, the tensile stress at the crown between the opposite CPs reduces to zero (dark blue area). The maximum principal tensile stress at the crown between the two dark blue areas is increased to 1.4MPa, as shown in Figure 10 (right).

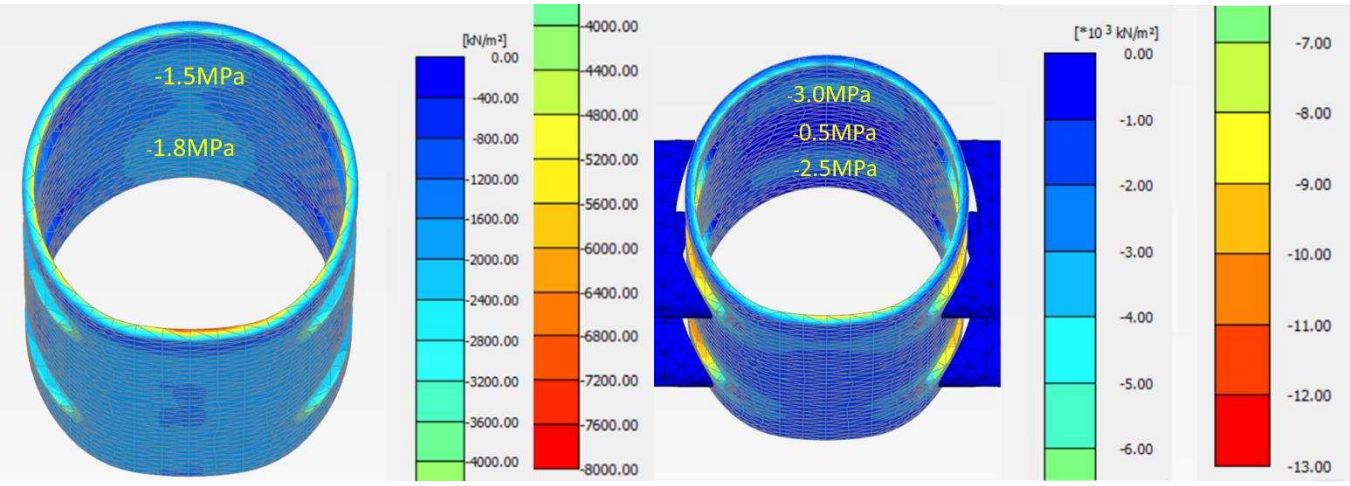

Figure 9: Principal compressive stress plot for model no.1 (thickening layer installed with primary layer, no EAT & SHK)

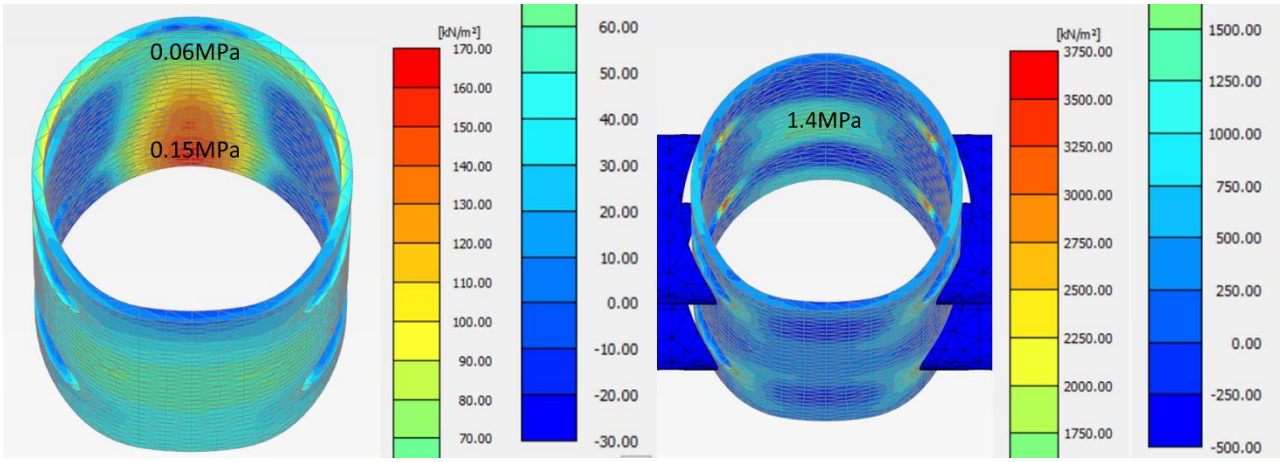

Figure 10: Principal tensile stress plot for model no.2 (thickening layer installed after the primary layer, no EAT & SHK)

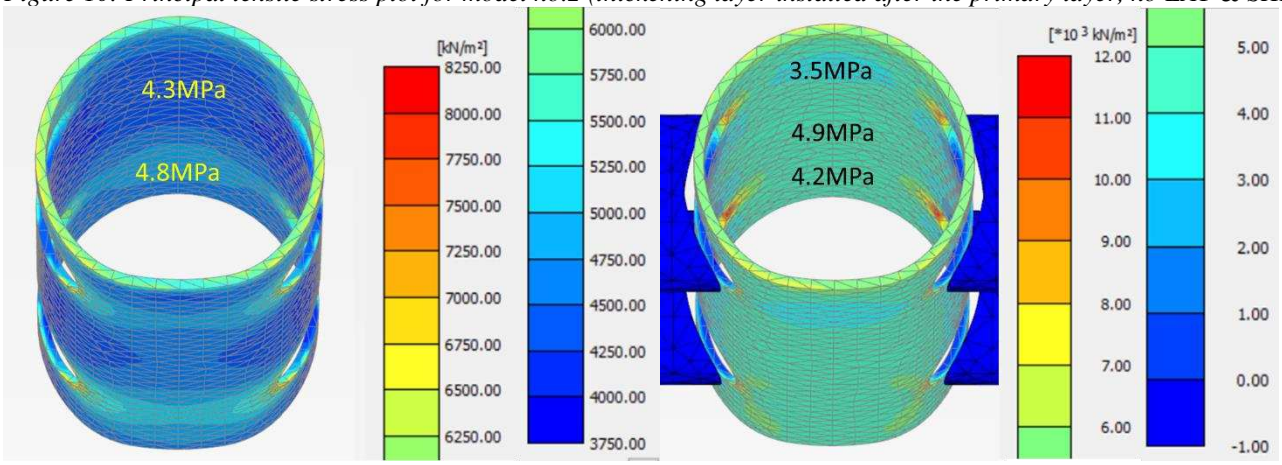

Figure 11: Principal tensile stress plot for model no.3 (thickening layer installed after the primary layer, with EAT & SHK)

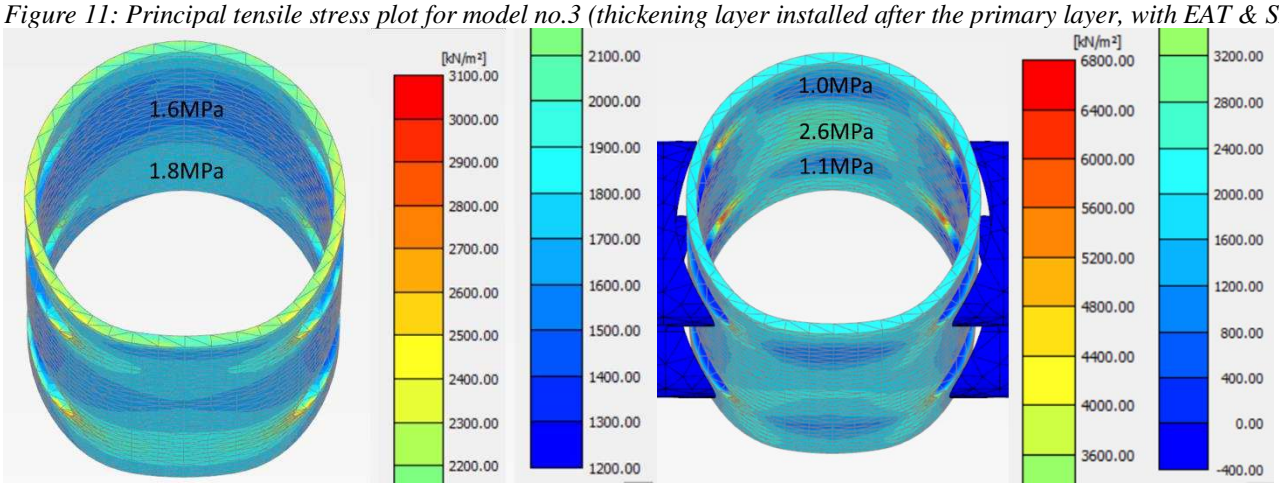

Figure 12: Principal tensile stress plot for updated model no.3 (with revised strain values for the EAT & SHK)

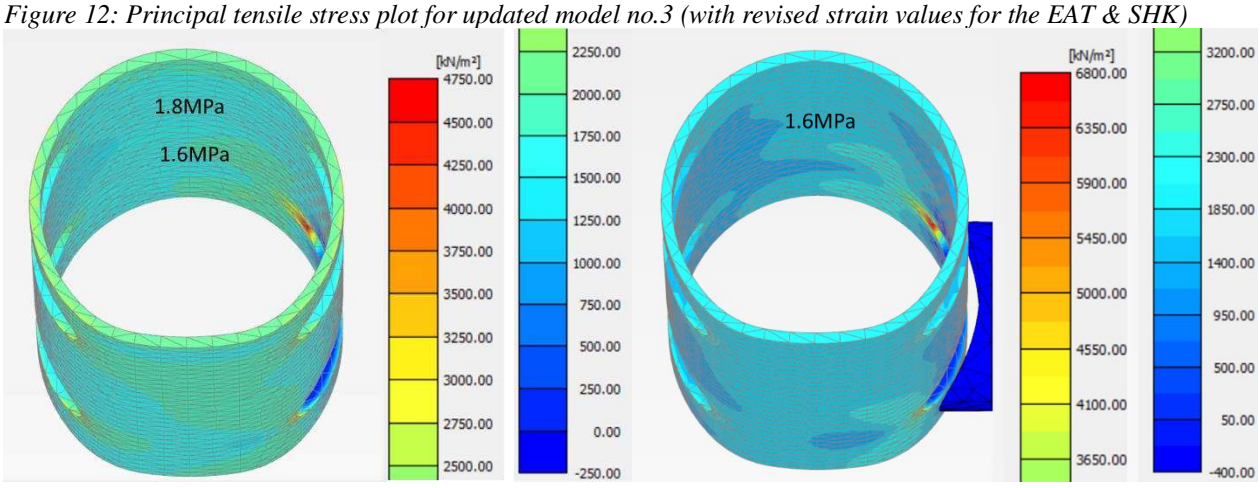

Figure 13: Principal tensile stress plot for single cross-passage case (with revised strain values for the EAT & SHK)

Figure 11 shows model no.3 principal tensile stress plots for the thickening layer including the effects of EAT & SHK, simulated by assigning 300 microstrains to the thickening layer. The principal tensile stress at the crown is around 4.3MPa and 4.8MPa for the stage before the CPs construction. After constructing CPs, the principal tensile stress at the crown is between 3.5MPa and 4.9MPa.

Crossrail SCL design specifies a maximum 28-day EAT&SHK strain at 300 microstrains, which was used as the input in the numerical model. However, part of the EAT&SHK strain occurs at the early age of the SCL, which has much less stiffness. Hence, the EAT&SHK generated stress should be less than the magnitude in the model. If the maximum principal tensile stress below 1.9MPa is assumed, the input strain value should be less than 110microstrain. Further numerical analysis for the model is undertaken with 110 microstrains inputs. The results are shown in Figure 12. It shows a maximum principal tensile stress around 1.8MPa and 2.6MPa at the stages before and after the CPs construction, matching the observation on site.

5.2 The impact of single and multiple CPs

An additional analysis was undertaken to investigate the impact of single and multiple CPs on the main tunnel lining performance. This analysis is based on model no.3 with revised 110 microstrains EAT & SHK. In this additional analysis, only the CP8 was constructed. CP8 is located further from the headwall, so its stiffening effect would not affect the analysis results.

Figure 13 shows the single CP case's total principal tensile stress results. It shows that the maximum total tensile stress both prior to and after the CP construction is around 1.6-1.8MPa at the centre line of the main tunnel thickening layer. This is much less than the maximum total tensile principal stress shown in Figure 12 (right), which is 2.6MPa. This shows the third limitation of the Crossrail junction design methodology and explains why “unexpected” cracks occurred at the crown.

5.3 Multiply CPs tunnel lining deformation

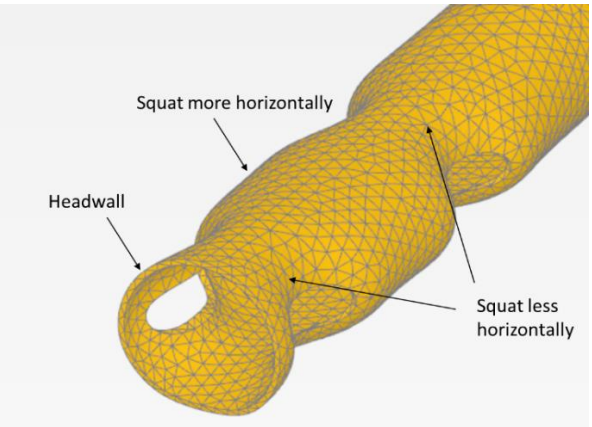

Figure 14: Deformed tunnel shape after the CPs construction

Figure 14 shows that the crown near the headwall location deforms the least. Hence, it takes less tensile stress than other crown areas. The tunnel crown between the opposite junctions is slightly flatter. This is because the breakout of the opening at the primary lining axis level reduces the ring stiffness. Therefore, the whole ring reduces size but can maintain its relative roundness. The tunnel crown between the four junctions squats more horizontally than any other place. Hence, more loads are resisted in the form of bending rather than axial force in this area, leading it more prone to lining cracks.

6 CONCLUSIONS

This paper investigates the contributing factor towards the longitudinal crack that occurred during the Crossrail Bond Street Station Concourse tunnel CH3 construction using finite element software PLAXIS 3D. The contributing factors of sequential construction of the thickening layer, the EAT&SHK effect in the thickening layer and the multiple CPs construction were included. It is found that all the above three factors should be included in the numerical analysis for more accurate prediction.

7 REFERENCES

Bloodworth, A., Su, J. 2018. Numerical analysis and capacity evaluation of composite sprayed concrete lined tunnels. *Underground Space*, 3(2), 87–108.

Crossrail. 2009. Civil Engineering Design Standard Part 7: Ground Movement Prediction.

Su, J. 2022a. Multi-layer lining design: a new framework for tunnel lining design, Tunnelling Journal, June/July 2022, 16-23.

Su, J., 2022b. Adopting “less is more” principle for efficient design of Composite SCL tunnels. Proceedings, ITA-AITES WTC2022, Copenhagen, Denmark.

Su, J. 2022c. Interpretation of fibre optic monitoring data from Crossrail Bond Street Station sprayed concrete lined (SCL) tunnel. Proceedings, 11th ISFMG. Imperial College London, London, United Kingdom.

Su, J., Bedi, A. 2019. Load-sharing effect for sprayed concrete lined tunnels in various ground conditions. Proceedings, XVII ECSMGE-2019. Reykjavik, Iceland.

Su, J., Bloodworth, A. 2018. Numerical calibration of mechanical behaviour of composite shell tunnel linings. *Tunnelling and Underground Space Technology*, 76, 107-120.

Su, J., Bloodworth, A. 2019. Simulating composite behaviour in SCL tunnels with sprayed waterproofing membrane interface: A state-of-the-art review. *Engineering Structures*, 191, 698-710.

Su, J., Thomas, A., 2015. Design of Sprayed Concrete Linings in Soft Ground—A Crossrail Perspective. In Crossrail Project: Infrastructure design and construction (Eds: by Black, M., Dodge, C. & Lawrence, U.), pp. 123-136. ICE Publishing, London, United Kingdom.